Recognition of exchange striction as the origin of magnetoelectric coupling in multiferroics

G. Yahia,[1,2] F. Damay,[3] S. Chattopadhyay,[4,5] V. Balédent,[1] W. Peng,[1] E. Elkaim,[6] M. Whitaker,[7] M. Greenblatt,[7] M.-B. Lepetit,[8,9] and P. Foury-Leylekian[1]

[1]*Laboratoire de Physique des Solides, CNRS, Univ. Paris-Sud, Université Paris-Saclay 91405 Orsay Cedex, France*

[2]*Laboratoire de Physique de la Matière Condensée, Université Tunis-El Manar, 2092 Tunis, Tunisia*

[3]*Laboratoire Léon Brillouin, CEA-CNRS UMR12 91191 Gif-sur-Yvette Cedex, France*

[4]*Université Grenoble Alpes, INAC-MEM, F-38000 Grenoble, France*

[5]*CEA-Grenoble, INAC-MEM, F-38000 Grenoble, France*

[6]*Soleil synchrotron, 91191 Gif-sur-Yvette Cedex, France*

[7]*Department of Chemistry and Chemical Biology, Rutgers, the State University of New Jersey, Piscataway, New Jersey 08854, USA*

[8]*Institut Néel, CNRS UPR 2940, 25 av. des Martyrs, 38042 Grenoble, France*

[9]*Institut Laue Langevin, 72 av. des Martyrs, 38042 Grenoble, France*

(Received 5 October 2016; published 31 May 2017)

The magnetoelectric coupling, a phenomenon inducing magnetic (electric) polarization by application of an external electric (magnetic) field and first conjectured by Curie in 1894, is observed in most of the multiferroics and used for many applications in various fields such as data storage or sensing. However, its microscopic origin is a long-standing controversy in the scientific community. An intense revival of interest developed in the beginning of the 21st century due to the emergence of multiferroic frustrated magnets in which the ferroelectricity is magnetically induced and which present an inherent strong magnetoelectric coupling. The Dzyaloshinskii-Moriya interaction (DMI) well accounts for such ferroelectricity in systems with a noncollinear magnetic order such as the $RMnO_3$ manganites. The DMI effect is, however, inadequate for systems presenting ferroelectricity induced by quasicollinear spin arrangements such as the prominent RMn_2O_5 manganites. Among different microscopic mechanisms proposed to resolve this incompatibility, the exchange-striction model stands as the most invoked candidate. In this scenario, the polar atomic displacements originate from the release of a frustration caused by the magnetic order. Despite its theoretical description 15 years ago, this mechanism had yet to be unambiguously validated experimentally. The breakthrough finally comes from $SmMn_2O_5$ presenting a unique magnetic order revealed by powder neutron diffraction. The unique orientation of its magnetic moment establishes the missing element that definitely validates the exchange striction as the effective mechanism for the spin-induced ferroelectricity in this series. More generally, this is a proof of concept that validates this model on actual systems, facilitating the development of a new generation of multiferroics with unrivaled magnetoelectric properties.

DOI: 10.1103/PhysRevB.95.184112

I. INTRODUCTION

Magnetoelectric multiferroics, which couple simultaneous ferroelectric and magnetic orders, present an unrivaled interest due to their strong magnetoelectric coupling (MEC) [1,2]. They indeed offer, for instance, the opportunity to write a magnetic information by application of a small electric voltage, thus strongly reducing the energy consumption during data storage. Maximizing the cross-coupling between ferroelectricity and magnetism is thus of great importance for technological applications.

In this context, magnetically induced ferroelectrics attract much attention for their inherent MEC. In order to conceive new, optimized, spin-induced bulk multiferroics, one needs to elucidate the fundamental and challenging issue of the microscopic origin of the spin-induced ferroelectricity. The mechanism which has been first proposed is based on a spin current [3] involving antisymmetric DMI between noncollinearly ordered spins. Indeed, the DMI favors the displacement of the ligand anions from the bond axis between two magnetic sites. For some magnetic orders, such as the cycloids observed in the well-known hexagonal $RMnO_3$ manganites, such displacements lead to a macroscopic electric polarization [4,5]. In orthorhombic $RMnO_3$, another mechanism called exchange striction (ES) is able to explain the electric polarization from a collinear magnetic order [6–8]. Recently, a new family of manganites RMn_2O_5 has renewed the interest for ES mechanism because, in $TbMn_2O_5$ [9] and $GdMn_2O_5$[10], the electric polarization has been totally reversed via a modest magnetic field, revealing a strong magnetoelectric coupling. This is particularly interesting, since it is known that $GdMn_2O_5$ presents the most important polarization reported ($P_b > 3600\ \mu C\,m^{-2}$) [10]. The quasicollinear character of the magnetic ordering in the RMn_2O_5 [9] family renders the DM scenario unlikely, which opened an intense debate concerning the microscopic origin of the strong MEC in the RMn_2O_5 series [11], reinforced by the recent discovery of a room temperature preexisting polarization [12]. An emerging model has been first proposed in Refs. [13,14]. It involves an exchange-striction (ES) scenario [15,16], in which a structural relaxation induced by the relaxation of competing Heisenberg terms creates polar atomic displacements. However, an experimental evidence is still missing to assess this scenario in this family.

Until now, the multiferroic behaviors observed for the various compounds of the RMn_2O_5 series were different, but with common magnetic orders. Compounds with large ionic radii R, as La and Pr do not present a detectable electric polarization and can be considered as paraelectric [17], while Sm, Eu, and smaller rare earths present a finite polarization along the *b* crystallographic axis. The intermediate size member $NdMn_2O_5$

shows only a minute polarization, two orders of magnitude weaker than those of Sm or Eu compounds [18,19]. The size of R also affects the magnetic ordering characteristics. All members with small ionic radii rare earths [$Z > 64$ (Gd)], which are ferroelectric, undergo the same series of transitions: (i) a paramagnetic to an incommensurate magnetic (ICM_1) transition at T_1, (ii) an ICM to commensurate magnetic (CM) order at T_2 (usually associated with the ferroelectric transition), (iii) a transition to another incommensurate order (ICM_2) at T_3, and (iv) ultimately a possible transition ascribed to rare earth ordering. But for all of the RMn_2O_5, the magnetic moments always lie in the (a,b) plane and with a quasicollinear spin alignment.

This universal magnetic behavior for all ferroelectric members of RMn_2O_5 is at the core of the difficulty of assessing an ES mechanism. This systematic behavior associated with a quasicollinearity of the spins is unfortunately not relevant to unequivocally validate any of the two magnetoelectric models. A compelling evidence would be a multiferroic compound with purely collinear moments. This case would definitely rule out the DM scenario and prove the validity of the ES mechanism. In this context, the compositions with intermediate R^{3+} size, such as R=Sm and Gd, present a great interest from their key position between ferroelectric and nonferroelectric compounds, sustained by the discovery in $GdMn_2O_5$ of a surprisingly large polarization [10] for the series. However, their magnetic structure determination has been complicated by the strong neutron absorption cross section of both Gd and Sm. In $SmMn_2O_5$, heat capacity measurements have evidenced three λ-like anomalies at $T_1 = 35 \pm 2$ K, $T_2 = 28 \pm 2$ K, and $T_3 = 6 \pm 2$ K [20]. At T_1 and T_2, diverging peaks are observed in the thermal variation of the dielectric constant [21]. They correspond to the appearance of a weak electric polarization below T_1, strongly enhanced below T_2. Moreover, T_1 coincides with an anomaly in the magnetic susceptibility along the a direction [21], while T_2 corresponds to a significant decrease of the magnetic susceptibility along the c direction. T_3 corresponds to a broad upturn of the magnetic susceptibility along the c axis, with a weak impact along the a direction, evidencing complex magnetic behaviors. In addition, recent magnetic x-ray diffraction studies have been performed [10,22]. They have shown the participation of both the manganese and rare earth moments to the magnetic order. However, these measurements were not able to give details on the magnetic structure. The accurate direction of the moments, their amplitude, and couplings remained to be resolved.

To further understand the microscopic origin of the multiferroicity in the RMn_2O_5 family, we carried out an extensive investigation of $SmMn_2O_5$, including a neutron diffraction study. This work presents the accurate determination of its magnetic structure and shows that the spins are strictly coaligned along the c direction. The exact collinearity of the moments unambiguously and definitively shows that the ferroelectricity in the RMn_2O_5 family is driven by the exchange-striction model.

II. EXPERIMENTAL RESULTS

The measurements presented in this paper were performed on an isotope-enriched (^{154}Sm), high purity and high quality powder. The synthesis was carried out following the process described in Ref. [17], starting from a ^{154}Sm enriched Sm_2O_3 oxide.

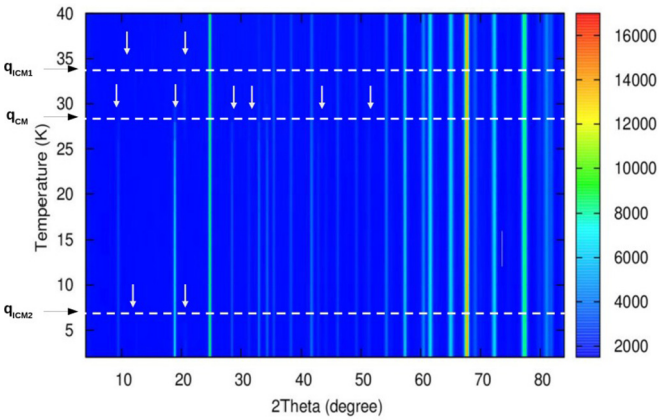

FIG. 1. Diffractograms as a function of the temperature of the powder neutron diffraction pattern of $SmMn_2O_5$ at 6 K. The white arrows indicate the new magnetic reflections associated with the various magnetic propagation wave vectors.

In order to study magnetostriction effects or structural distortions at the magnetic and dielectric transitions, a synchrotron radiation diffraction experiment has been performed on the CRISTAL beamline at the Soleil synchrotron light source (Saint-Aubin, France). The measurements were performed using a two-circles diffractometer, with 21 analyzer crystals to improve the angular resolution, and a short x-ray wavelength of 0.48 Å to reduce absorption effects. No symmetry lowering with respect to the average *Pbam* 300 K space group was detected at low temperature. Refinements of the structure between 10 and 40 K show that there is no significant variations in the positions of the Mn and Sm ions, when comparing with the 300 K structure. The thermal variation of the lattice parameters, extracted from the refinements, does not present any significant anomaly. The absence of lattice distortion, symmetry breaking, and lattice parameter modification in $SmMn_2O_5$ contrasts with the case of smaller R compounds. Indeed, in $TbMn_2O_5$, superstructure reflections as well as reflections associated with a symmetry breaking have been observed on single crystals [23] below T_2. The absence of significant structural effect at the ferroelectric transitions of $SmMn_2O_5$ is surprising, since the electric polarization is three times larger than in $TbMn_2O_5$. This is probably due to the lack of sensitivity of the measurements performed on powder.

Powder neutron diffraction experiments were carried out on a 2 g powder sample on the G4.1 diffractometer (Orphée-LLB, CEA-Saclay, France). The neutron wavelength was 2.426 Å. Measurements were performed by heating up the sample from 2 K to 300 K, with a step of 50 K above 50 K, and of 2 K below 40 K. The 1.5 K diffractogram is shown on Fig. 1. Refinements of the nuclear and magnetic structures were performed with the FULLPROF program [24]. Above a temperature very close to T_1, the neutron powder diffraction (NPD) pattern is very close to the one at 300 K. Below T_1, a few weak additional reflections are visible in the neutron diffractogram, but not in the x-ray one. This new set of reflections can be indexed with a propagation wave vector

$\mathbf{q}_{\mathrm{ICM1}} = [0.5\ 0\ 0.327(5)]$. Its components are close to the ones usually observed in the high temperature incommensurate phase of the RMn_2O_5 compounds with smaller R [14,25]. While the a^* component of q_{ICM1} is strictly commensurate, the c^* component is incommensurate but very close to $\frac{1}{3}$ and varies slightly with temperature between T_1 and T_2. Below a temperature close to T_2, the intensity of these reflections decreases, so that below 26 K they have totally vanished. Below T_2, several new reflections appear. This new set of reflections can be indexed with a commensurate magnetic propagation wave vector $\mathbf{q}_{\mathrm{CM}} = (0.5\ 0\ 0)$. The intensity develops quite abruptly as a function of the temperature: this observation, alongside the coexistence of $\mathbf{q}_{\mathbf{ICM1}}$ and $\mathbf{q}_{\mathbf{CM}}$ reflections, indicate a first order transition, in agreement with the thermal hysteresis on the susceptibility curve reported by [21] at this temperature. Finally, below a temperature close to T_3, two new reflections indexed with a propagation wave vector $\mathbf{q}_{\mathrm{ICM2}} = [0.5\ 0\ 0.335(5)]$ appear and coexist with the $\mathbf{q}_{\mathbf{CM}}$ reflections down to 1.5 K. It is interesting to note that (i) the intensity of the reflections of the CM phase remains constant below T_3 down to 1.5 K, which indicates a true coexistence with the $\mathbf{q}_{\mathrm{ICM2}}$ order, and (ii) the intensities of the magnetic reflections in both $\mathbf{q}_{\mathrm{ICM1}}$ and $\mathbf{q}_{\mathrm{ICM2}}$ phases are different, indicating that the T_3 transition is not a reentrance of the $\mathbf{q}_{\mathrm{ICM1}}$ phase.

III. SYMMETRY ANALYSIS AND REFINEMENT

Prior to the magnetic structure refinement, we used symmetry analysis of the system. Despite the fact that no symmetry lowering with respect to the $Pbam$ space group can be seen in the PND experiment, the existence of a polarization along **b** at low temperature as well as the results of Ref. [12] clearly state a lower symmetry space group (Pm following Ref. [12]). At this point one should remember that in quantum mechanics the (magnetic) space group of a system is defined as the space-time symmetry operations leaving its Hamiltonian invariant ($\mathcal{G} = \{g,\ g\hat{H} = \hat{H}g\}$). While describing a magnetic structure, the usage is rather to define the magnetic group as the symmetry operations leaving the magnetic pattern (the magnetic part of the wave function) invariant ($G = \{g,\ g\Psi_{GS} = \Psi_{GS}\}$). These two definitions are quite different since in the Hamiltonian group ($\mathcal{G}$) the ground-state wave function (Ψ_{GS}) may belong to any of the irreducible representations (irrep) of the group, and thus be symmetry related, but not invariant, under some symmetry operations. Let us first derive the Hamiltonian magnetic group $\mathcal{G}$. The all-electrons Hamiltonian includes the kinetic energy and electrons repulsion terms (invariant under all orthogonal transformations of space as well as the time inversion), the electron-nuclei attraction (invariant under Pm), and at least the spin-orbit coupling $\hat{H}_{SO}$. The magnetic group can thus be defined as the magnetic group issued from Pm and leaving also $\hat{H}_{SO}$ invariant. The rare-earth atoms R are located on the m mirror and should thus either belong to the m, m', or $m1'$ point group. One can show, with a bit of algebra, that while $g = m'$ commutes with $\hat{H}_{SO}$, this is neither the case for m and the time inversion τ. It results that the R point group should be m' and thus that the $SmMn_2O_5$ magnetic group $\mathcal{G} = Pm'$. At this point one should remember that neutrons see the magnetic moments correlation functions

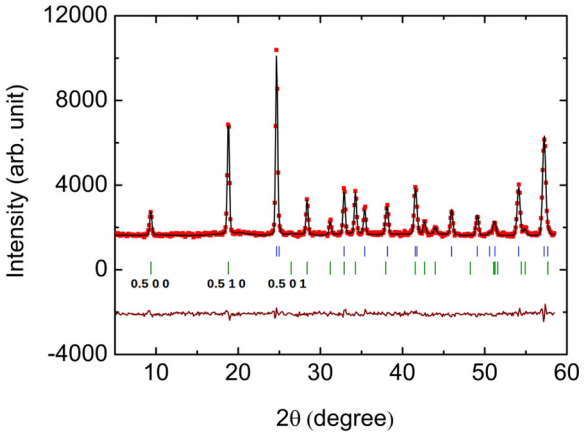

FIG. 2. Rietveld refinement of the neutron diffraction pattern. The experimental data are in red, the calculated profile in black, and their difference in blue. Green ticks indicate Bragg peak positions. The index of the first magnetic reflections is given.

that correspond in an antiferromagnetic (AFM) system to one of the Néel determinants in the singlet wave function. A $\mathbf{q}_{\mathrm{CM}} = (0.5\ 0\ 0)$ AFM propagation wave vector seen in neutron scattering thus corresponds for the ground state wave function to $\mathbf{q}^{\mathrm{GS}}_{\mathrm{CM}} = (0\ 0\ 0)$ and Ψ_{GS} belongs to one of the Γ point irreps. Nevertheless, for the sake of simplicity we will express the character table in the $P_{2a}m'$ Hamiltonian group (unique axis **c**) so that the symmetry of the Néel state will clearly appear. In this schema, the $P_{2a}m'$ group has four irreducible corepresentations (correp) of dimension 1 at the Γ point (see Supplemental Material [26] for the character table), yielding either to AFM or FM solutions along **a**, and moments either in the **(a,b)** plane or along the **c** direction for the R^{3+} and Mn^{3+} ions (the direction of the Mn^{4+} ions are not symmetry constrained). Let us note that totally symmetric irrep Γ_1 corresponds to an in-plane AFM order as found in the Tb, Ho, or Dy compounds [27].

Let us now focus on the 6 K commensurate magnetic structure determination using Rietveld refinement and symmetry adapted modes derived from representation analysis and the usual magnetic group convention. The $Pbam$ to Pm symmetry breaking being small, the further analysis of the spin order will be conducted using the $Pbam$ space group, in order to minimize the number of parameters. There are two irreducible representations of the little group G_k. The magnetic representations G_m calculated for the Wyckoff positions of the Sm^{3+}, Mn^{3+}, and Mn^{4+} sites ($4g$, $4h$, and $4f$), and considering the propagation vector $\mathbf{q}_{\mathrm{CM}} = (0.5\ 0\ 0)$, lead to $G_m = 3\Gamma_1 + 3\Gamma_2$ for Mn^{4+}, and $G_m = 2\Gamma_1 + 4\Gamma_2$ for Mn^{3+} and Sm^{3+}. The representations correspond to different spin orders of symmetry that correspond to different couplings of symmetry related pairs in the structure. Only the symmetry mode giving spins along the c axis for all the sites provide a good agreement with the experimental data, as illustrated by the Rietveld refinement of Fig. 2. The corresponding magnetic ordering is characterized by ferromagnetic pairs of Mn^{4+} along c, which are ferromagnetically coupled together within the (a,b) plane. For Mn^{3+}, there is an antiferromagnetic order relating (x,y,z) and $(-x,-y,z)$ and a ferromagnetic one

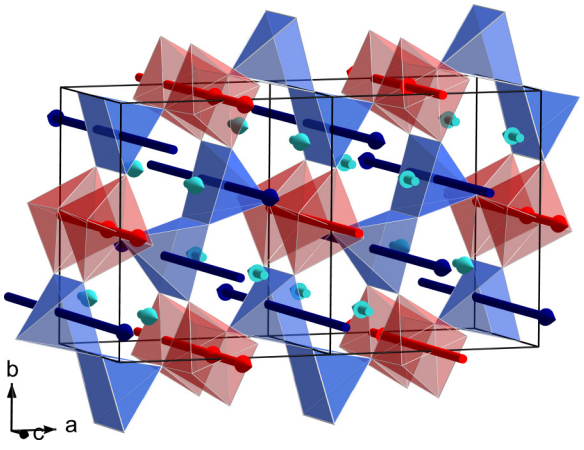

FIG. 3. Perspective view of the magnetic structure of $SmMn_2O_5$ at 6 K. The blue Mn^{3+} pyramids and the red Mn^{4+} octahedra are represented.

relating $(-x+1/2, y+1/2, -z$ and $x+1/2, -y+1/2, -z)$. Most strikingly, in $SmMn_2O_5$, all moments are parallel to c, a feature contrasting with the ususal ab plane anisotropy of the magnetic moments in the other R members of the series, either with smaller or larger R^{3+} size. The magnetic ordering is illustrated on Figs. 3 and 4. Note that the refinement is significantly improved when one introduces a partial order of the Sm^{3+} spins (see Table I and Fig. 2), with a moment refined to $0.43\mu_B$, also along c. The thermal variation of the amplitude of the moments deduced from the refinement at various temperatures in the CM phase (see Supplemental Material [26] for the temperature evolution of the magnetic moments in Fig. 1) emphasizes the fact that the contribution of the Sm, although very weak ($0.2\mu_B$) is already present at T_2 and progressively increases with decreasing temperature. This feature is however not unique in this series. In $TbMn_2O_5$ and $HoMn_2O_5$, a partial ordering of the R^{3+} moments has been observed as high as 26 K [27]. The magnetic ordering modeled from the neutron diffraction data at 6 K matches the model proposed by Ishii *et al.* [22]. The only difference lies

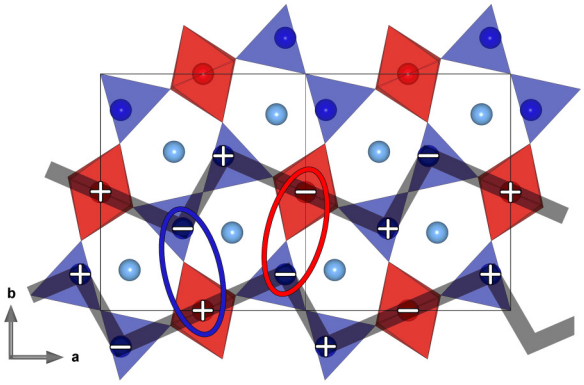

FIG. 4. Projection in the (a,b) plane of the magnetic moments along c represented by + and − symbols. The gray lines represent the AFM chains coupled through the J_3 magnetic integrals (represented as red and blue circles: red for FM order; blue for AFM order). The encircled red and blue J_3 couplings are related by the $a\ x, 1/4, z$ symmetry operation within the $Pbam$ space group.

TABLE I. Magnetic structure parameters of $SmMn_2O_5$ at 30 K for $q_{ICM1} = (0.5\ 0\ 0.327)$. $\Phi = \widehat{\vec{M},\vec{a}}$.

	x/a	y/b	z/c	Φ (deg)	M(μ_B)
Sm^{3+}	0.36	0.67	0	0	0.225
Mn^{3+}	0.401	0.347	0.5	20.708	−2.619
Mn^{4+}	0	0.5	0.252	20.708	0.999

in the direction along c of the moments for one pair of Sm^{3+}, which is reversed in our present case, with respect to the result of Ref. [22].

Comparing this magnetic structure with the correp of the Hamiltonian group $P_{2a}m'$ (see Supplemental Material [26] for the character table), one sees immediately that it belongs to the Γ_3 correp. Going now back to the magnetic group definition defined previously, one sees that the only possible symmetry operations issued from $Pbam$ and the time-inversion τ are $G = \{E, t'_a, m, m \circ t'_a\} = P_{2a}m$, which defines the magnetic space group of $SmMn_2O_5$ in its commensurate phase.

Below 6 K, two broad reflections appear at incommensurate positions. Their presence does not affect the intensity of the existing magnetic Bragg peaks. They are likely connected to a further ordering of the Sm moments, involving arguably an incommensurate modulation of their amplitude, or of their orientation with regards to the c axis.

This low temperature $\mathbf{q}_{ICM1}$ phase is very difficult to study because it involves only two very weak reflexions on the neutron powder diffractograms, thus offering a vast number of possible magnetic models. To improve the reliability of our modelings, we have tried magnetic configurations keeping the same magnetic orders between Mn^{3+} and Mn^{4+} pairs. Our best attempts suggest that, in this $\mathbf{q}_{ICM1}$ phase, Mn^{3+} and Mn^{4+} moments are roughly aligned along the a direction, like in the other RMn_2O_5 compounds. A contribution of the Sm moments can also be refined.

IV. DISCUSSION

In comparison with the other members of the series, the magnetic structure of $SmMn_2O_5$ in the commensurate phase presents some fundamental differences which are important to properly address. The first one concerns the c^* component of the propagation wave vector which strongly differs from the value of $1/4$ usually observed in the series. The c^* component of the propagation wave vector is known to depend on the nature of R: its size and its number of $4f$ electrons. However, a ferromagnetic ordering along the c direction has never been observed in this series, except for $PrMn_2O_5$. It indicates that the effective exchange coupling between the Mn^{4+} through the Mn^{3+} and R^{3+} planes is always ferromagnetic [17]. The most striking difference is, however, the alignment of the moments along the c direction in the CM ferroelectric phase. Indeed, $SmMn_2O_5$ is exceptional in the series, since all the other members present magnetic moments within the (a,b) plane.

To understand the importance of such a result, we need to emphasize several details on the two main models, namely the DMI and ES models discussed in the Introduction. On one hand, the DMI allows the magnetic order to induce an electric

polarization only if the spins are not perfectly collinear. The induced polarization can then be expressed as a function of the cross product between first neighbors spins: $P \propto \vec{S}_i \wedge \vec{S}_j$. Due to this vectorial nature, any change in the spins directions results in a change in the polarization. Since all the members of the family (except $SmMn_2O_5$) present not fully parallel moments in the (a,b) plane, and a polarization along the b axis, this model could not be excluded. In the $SmMn_2O_5$ compound, however, the magnetic moments are perfectly aligned, and thus the DMI cannot explain the existence of an electric polarization and even less its exceptionally large magnitude. On the other hand, ferroelectricity induced by ES can be expressed as a scalar product between neighboring spins: $P \propto \vec{S}_i.\vec{S}_j$, maximal for perfectly parallel moments as found in the $SmMn_2O_5$ compound. Let us remember that the exchange-striction model is based on the lowering of the magnetic energy by lifting the equality of the four magnetic exchange terms involving J_3 within a unit cell. Indeed, due to the opposite signs of the $\langle S_i \cdot S_j \rangle$ involving J_3, its contribution is null within the unit cell for the $Pbam$ group symmetry (see Fig. 4) but not in the Pm symmetry. In order to increase/decrease the J_3 amplitude one has to act on the AFM/FM coupled spins and thus increase AFM/FM aligned spins. In this aim one needs to increase/decrease the Mn_1–O_4–Mn_2 angle (see coupling analysis of Ref. [28]). The involved atomic movements are (quasi-) related by the $a\ x,1/4,z$ symmetry operation resulting in a global electric polarization essentially along the b direction. All this analysis applied in the particular case of $SmMn_2O_5$ enables us to unambiguously conclude that the mechanism responsible for the spin-induced electric polarisation in the entire RMn_2O_5 series is the ES model.

V. CONCLUSIONS

In summary, we report an accurate magnetic structure of $SmMn_2O_5$ in the ferroelectric phase deduced from neutron diffraction experiment. In contrast to other RMn_2O_5 compounds, $SmMn_2O_5$ exhibits perfectly collinear moments oriented along the c axis. This unique property constitutes the missing fingerprint to unambiguously assert that exchange striction applies to RMn_2O_5 and explains the strong polarization of the compound. This breakthrough in the understanding of the RMn_2O_5 series gives a robust and universal starting point to investigate more advanced concepts such as the electromagnon, a mysterious manifestation of the magnetoelectric coupling in the dynamical channel.

ACKNOWLEDGMENTS

We would like to thank L. Chapon for very fruitful discussions. This work was supported by project CMCU PHC UTIQUE 15G1306. The work of M.G. was supported by NSF-DMR Grant No. 1507252.

[1] W. Eerenstein, N. D. Mathur, and J. F. Scott, Nature (London) **442**, 759 (2006).
[2] T. Lottermoser *et al.*, Nature (London) **430**, 541 (2004).
[3] H. Katsura, N. Nagaosa, and A. V. Balatsky, Phys. Rev. Lett. **95**, 057205 (2005).
[4] I. A. Sergienko and E. Dagotto, Phys. Rev. B **73**, 094434 (2006).
[5] Y. Tokura *et al.*, Adv. Mater. **22**, 1554 (2010).
[6] A. Munoz, M. T. Casais, J. A. Alonso, M. J. Martinez-Lope, J. L. Martinez, and M. T. Fernandez-Diaz, Inorg. Chem. **40**, 1020 (2001).
[7] B. Lorenz, Y.-Q. Wang, and C.-W. Chu, Phys. Rev. B **76**, 104405 (2007).
[8] V. Yu. Pomjakushin, M. Kenzelmann, A. Dönni, A. B. Harris, T. Nakajima, S. Mitsuda, M. Tachibana, L. Keller, J. Mesot, H. Kitazawa, and E. Takayama-Muromachi, New J. Phys. **11**, 043019 (2009).
[9] N. Hur, S. Park, P. A. Sharma, J. S. Ahn, S. Guha, and S-W. Cheong, Nature (London) **429**, 392 (2004).
[10] N. Lee, C. Vecchini, Y. J. Choi, L. C. Chapon, A. Bombardi, P. G. Radaelli, and S-W. Cheong, Phys. Rev. Lett **110**, 137203 (2013).
[11] S. W. Cheong and M. Mostovoy, Nat. Mater. **6**, 13 (2007).
[12] V. Balédent, S. Chattopadhyay, P. Fertey, M. B. Lepetit, M. Greenblatt, B. Wanklyn, F. O. Saouma, J. I. Jang, and P. Foury-Leylekian, Phys. Rev. Lett. **114**, 117601 (2015).
[13] I. Kagomiya, S. Matsumoto, K. Kohn, Y. Fukuda, T. Shoubu, H. Kimura, Y. Noda, and N. Ikeda, Ferroelectrics **286**, 167 (2003).
[14] L. C. Chapon, G. R. Blake, M. J. Gutmann, S. Park, N. Hur, P. G. Radaelli, and S.-W. Cheong, Phys. Rev. Lett. **93**, 177402 (2004).
[15] L. C. Chapon, P. G. Radaelli, G. R. Blake, S. Park, and S.-W. Cheong, Phys. Rev. Lett. **96**, 097601 (2006).
[16] B. Kh. Khannanov, E. I. Golovenchits, and V. A. Sanina, J. Phys.: Conf. Ser. **572**, 012046 (2014).
[17] C. Doubrovsky, G. André, A. Gukasov, P. Auban-Senzier, C. R. Pasquier, E. Elkaim, M. Li, M. Greenblatt, F. Damay, and P. Foury-Leylekian, Phys. Rev. B **86**, 174417 (2012).
[18] I. Kagomiya, K. Kohn, and T. Uchiyama, Ferroelectrics **280**, 131 (2002).
[19] S. Chattopadhyay, V. Balédent, F. Damay, A. Gukasov, E. Moshopoulou, P. Auban-Senzier, C. Pasquier, G. André, F. Porcher, E. Elkaim, C. Doubrovsky, M. Greenblatt, and P. Foury-Leylekian, Phys. Rev. B **93**, 104406 (2016).
[20] M. Tachibana, K. Akiyama, H. Kawaji, and T. Atake, Phys. Rev. B **72**, 224425 (2005).
[21] T. Fujita and K. Kohn, Ferroelectrics **219**, 155 (1998).
[22] Y. Ishii, S. Horio, M. Mitarashi, T. Sakakura, M. Fukunaga, Y. Noda, T. Honda, H. Nakao, Y. Murakami, and H. Kimura, Phys. Rev. B **93**, 064415 (2016).
[23] J. Koo, C. Song, S. Ji, J.-S. Lee, J. Park, T.-H. Jang, C.-H. Yang, J.-H. Park, Y. H. Jeong, K.-B. Lee, T. Y. Koo, Y. J. Park, J.-Y. Kim, D. Wermeille, A. I. Goldman, G. Srajer, S. Park, and S.-W. Cheong, Phys. Rev. Lett. **99**, 197601 (2007).
[24] J. Rodriguez-Carvajal, Physica B **192**, 55 (1993).

[25] G. Buisson, Phys. Status Solidi **16**, 533 (1973); **17**, 191 (1973); P. G. Radaelli and L. C. Chapon, J. Phys.: Condens. Matter **20**, 434213 (2008).

[26] See Supplemental Material at http://link.aps.org/supplemental/10.1103/PhysRevB.95.184112 for the character table of the symmetry group for $SmMn_2O_5$ and the temperature evolution of the magnetic moments.

[27] G. R. Blake, L. C. Chapon, P. G. Radaelli, S. Park, N. Hur, S.-W. Cheong, and J. Rodriguez-Carvajal, Phys. Rev. B **71**, 214402 (2005).

[28] S. Petit, V. Balédent, C. Doubrovsky, M.-B. Lepetit, M. Greenblatt, B. Wanklyn, and P. Foury-Leylekian, Phys. Rev. B **87**, 140301(R) (2013).